Carb liquid-scintillation spectrometer. The efficiency of counting was determined with tritiated toluene as the internal standard. Synthesis of protein and collagen was measured just before the addition of thymidine to show that synthesis was going on during the FUdR block and to demonstrate the rate of synthesis.

In the aneuploid mouse line (Fig. 1), a burst of DNA synthesis begins immediately after the FUdR block is reversed and reaches a maximum in 4 to 6 hours. Protein synthesis is only moderately changed, increasing slightly during the first part of S from the rate prior to release of the block. Collagen synthesis also increases slightly, approximating the changes in general protein synthesis. In these aneuploid cells, therefore, specialized protein synthesis is not shut off or decreased during the S period.

To determine whether the control of synthesis of collagen in diploid cells is different from that of aneuploid cells, similar experiments were performed with diploid rat (PR105) and diploid fetal human (PR100) cell lines. Cells of PR105 make 10 percent of total protein as collagen, whereas 3.5 percent is the highest we have obtained with the aneuploid cells (3T6). In Fig. 2 a sharp burst of DNA synthesis is seen in cultures of PR105, with a peak at 3 to 4 hours after reversal of FUdR block. The rate of incorporation of proline into protein increases moderately from the level prior to addition of thymidine and the changes in collagen synthesis follow closely the changes in protein synthesis, as found for 3T6 cells. In the cultures of diploid fetal human cells (Fig. 3), synthesis of DNA was maximum 3 to 5 hours after addition of thymidine. Protein synthesis fluctuated, but showed a slight tendency to decrease during maximum DNA synthesis. Changes in collagen synthesis are again similar to those in protein synthesis.

Stollar, Buonassisi, and Sato (*17*) noted that synthesis of adrenal steroids per unit number of cultured adrenal tumor cells remained unchanged in logarithmic and stationary phases of growth. We have shown (*18*) that synthesis of collagen per unit number of cells in culture fluctuates with general protein synthesis during the logarithmic and stationary phases of growth and is more rapid during the logarithmic phase. Our results indicate that production of collagen does not cease during that portion of the cellular division cycle when DNA is replicated, but instead that it again fluctuates with changes in general protein synthesis. Moreover, aneuploid and diploid cells respond similarly. In both types of cultures the rate of transcription of collagen appears to be controlled by a mechanism that alters the rate of transcription of all proteins.

LOIS M. DAVIES*
JEAN H. PRIEST
ROBERT E. PRIEST
Department of Pathology, University of Colorado Medical Center, Denver

References and Notes

1. A. Marchok and H. Herrman, *Bull. Inst. Cell. Biol.* **7**, No. 6 (1966); C. Grobstein, in *The Cell*, J. Brachet and A. F. Mirsky, Eds. (Academic, New York, 1959), vol. 4, p. 437.
2. H. Holtzer, J. Marshall, H. Fink, *J. Biophys. Biochem. Cytol.* **3**, 705 (1957); F. Stockdale and H. Holtzer, *Exp. Cell Res.* **24**, 508 (1961).
3. N. K. Wessells, *J. Cell Biol.* **20**, 415 (1964).
4. O. Mäkelä and G. Nossal, *J. Exp. Med.* **115**, 231 (1962).
5. J. Papaconstantinou, *Amer. Zool.* **4**, 279 (1964); T. Yamada and C. Takata, *J. Cell. Biol.* **27**, 114A (1965); C. Takata, J. Albright, T. Yamada, *Science* **147**, 1299 (1965).
6. H. Goldberg, H. Green, C. Todaro, *Exp. Cell Res.* **31**, 444 (1963).
7. H. Goldberg and H. Green, *J. Cell Biol.* **22**, 227 (1964).
8. Supplied by Dr. H. Green, Dept. of Pathology, New York University.
9. M. R. Stetten and R. J. Schoenheimer, *J. Biol. Chem.* **153**, 113 (1944).
10. M. A. Rich, J. L. Bolaffi, J. E. Knoll, L. Cheong, M. L. Eidinoff, *Cancer Res.* **18**, 730 (1958); J. W. Littlefield, *Exp. Cell Res.* **26**, 318 (1962); J. H. Priest, J. E. Heady, R. E. Priest, *J. Nat. Cancer Inst.* **38**, 61 (1967).
11. This medium represents an enrichment of Eagle's basal medium; it was formulated by Dr. R. Dulbecco, Salk Institute for Biological Studies, San Diego, California. The composition is found in H. Ginsburg, in *Methodologic Approaches to the Study of Leukemias*, V. Defendi, Ed. (Wistar Inst. Press, Philadelphia, 1965).
12. R. Ham, *Exp. Cell Res.* **29**, 515 (1962). This medium contains both thymidine and proline, which were omitted individually from media containing the respective radioactive element. In addition, during the time of FUdR block, the cells were incubated in medium without thymidine.
13. J. H. Priest, J. E. Heady, R. E. Priest, *J. Nat. Cancer Inst.* **38**, 61 (1967).
14. J. M. Reiter and J. W. Littlefield, *Biochem. Biophys. Acta* **80**, 562 (1964).
15. Radioactivity does not appear in hydroxyproline-containing protein until 30 minutes after addition of labeled proline, and the rate of incorporation does not parallel the rate of incorporation into the general cellular proteins until 3 hours. (R. E. Priest and L. M. Davies, *J. Cell Biol.*, in press.) The radioactive exposure time, then, is limited by the need for a short exposure to labeling material in synchrony experiments and by the length of time necessary to get sufficient radioactive incorporation into collagen.
16. K. Juva and D. W. Prockop, *Anal. Biochem.* **15**, 77 (1966). Total radioactive incorporation was assumed to represent proline in protein, and proline and hydroxyproline in collagen. Calculations were made according to H. Green and B. Goldberg, *Nature* **200**, 1097 (1963), to arrive at figures for noncollagenous protein synthesis and for collagen synthesis.
17. V. Stollar, V. Buonassisi, G. Sato, *Exp. Cell Res.* **35**, 608 (1964).
18. L. M. Davies and R. E. Priest, *Fed. Proc.* **26**, 300 (1967).
19. Supported by grant HE 08072 from USPHS. We thank H. Daniels for technical assistance.
* Present address: Department of Biology, Massachusetts Institute of Technology, Cambridge 02139.

13 November 1967

Isotope Separation by Carrier Diffusion

Abstract. *Nitrogen isotope fractionation in the Hoering-Moore experiment, injection of N_2 into CO_2 carrier and flow through sandstone, is due to diffusion in the gas phase rather than to surface interaction. This process, called "carrier diffusion," produces a characteristic fractionation pattern relative to a fraction coordinate, with points of zero fractionation at 16 and 84 percent and heavy isotope enrichment between these points. Carrier diffusion is an efficient enrichment process for low-abundance isotopes lighter than the abundant species and for helium and hydrogen in gas mixtures.*

Diffusional separation processes for gaseous and isotopic mixtures are of two general types: those which do not require an additional gas as a separating agent and those in which separation of the mixture occurs by diffusion through an added gas component. The first type includes the well-known process of barrier diffusion or effusion, characterized by molecular flow through a porous barrier, and the method of thermal diffusion across a temperature gradient. Processes which depend on a third component include mass diffusion (*1*), in which the mixture and a separating agent flow in opposite directions separated by a filter through which they interdiffuse, and sweep diffusion (*2*) in which a separating agent diffuses across the flowing mixture and sweeps the less-diffusible component to one side of the stream. Both mass and sweep diffusion operate with continuous flow of mixture through the separation unit and depend upon differential rates of diffusion perpendicular to the direction of flow. In this paper a one-dimensional separation process is described, in which a mixture is injected as a spike or batch into a flowing carrier gas and diffuses up and down stream from the injection point during the bulk flow. This process, called *carrier diffusion*, accounts for the nitrogen isotope separation observed in geochemical studies of gas flow in sandstones (*3*) and is applicable to unusual isotope effects observed in gas-solid chromatography (*4*) and to separation of gas mixtures in general.

In their experimental study, Hoering and Moore (*3*) injected N_2 into CO_2 flowing through a dry core of Torpedo sandstone and found that the emerging N_2 first increased and then decreased in

N^{15} content. Fractionation factors calculated according to conventional Rayleigh treatment were highly variable, which led them to propose a combination of molecular flow (with an effusive separation factor equal to the square root of the 29/28 ratio), viscous flow, and surface interaction effects, acting in combination to produce the experimental effects and possibly causing the isotopic variations in natural gas N_2 which they had observed.

The carrier diffusion process in simplest form is applied to a natural isotopic mixture in which one isotopic species is of very low abundance; the subscript "i" always designates this low-abundance species regardless of the sign of the mass difference relative to the abundant species (non-subscripted). The mixture is injected into a carrier gas as a spike at a point $x = 0$ in a one-dimensional moving coordinate system which has the bulk flow velocity of the carrier gas in the column. The volume concentration of the abundant isotopic species, C, in this coordinate system is:

$$C = \frac{N^\dagger}{2(\pi D t)^{\frac{1}{2}}} \exp[-z^2] \quad (1)$$

$$z = x/2(Dt)^{\frac{1}{2}} \quad (2)$$

D is the binary diffusion coefficient for the abundant species and carrier gas; $N^\dagger$ is the total number of moles of abundant species injected in the spike. $N^\dagger/2(\pi Dt)^{1/2} = C_0$, the concentration at $x = 0$, which decreases with time.

The distribution of the abundant isotope along x at any given time is described by a running variable f, the fraction of the total moles of this species which lies between $(-\infty)$ and x. The sign convention is that the bulk flow is toward $x = (-\infty)$, so that f increases from 0 to 1 as x (and z) range from $(-\infty)$ to $(+\infty)$, and measures the fraction of the mixture which has emerged from the column at any time. Integrating $C dz$ from $(-\infty)$ to z at a given time defines z in terms of this fraction as

$$z = -erf^{-1}(1 - 2f) \quad (3)$$

the function in Eq. 3 being the inverse error function. The fraction of total gas which is between two points x_1 and x_2 at any time is $f_2 - f_1 = (erf\ z_2 - erf\ z_1)/2$, while the fraction between the injection point, $z = 0$, and point z is simply $erf\ z/2$. When the rare isotope is in low abundance, as is assumed here, f may be taken as the fraction of the total mixture.

The isotopic ratio in the mixture is always defined as $C_i/C = R$, the ratio of rare to abundant species; from Eq. 1 this ratio is

$$\frac{R(x,t)}{R^\dagger} = \left(\frac{D}{D_i}\right)^{1/2} \exp\left[-\left(\frac{D}{D_i} - 1\right) z^2\right] \quad (4)$$

which, with Eq. 3, defines the ratio variation along f at any time. $R^\dagger$ is $(N_i^\dagger/N^\dagger)$, the mean ratio in the total mixture, and D_i is the diffusion coefficient for the rare isotopic species. In this report it is assumed that the mixture is in low enough concentration in the carrier gas that D_i can be taken as the binary diffusion coefficient between the rare isotopic species and the carrier gas. Ratio variations are described by the variables $\lambda = \ln(R/R^\dagger)$ and $\delta = (R/R^\dagger) - 1$ which are approximately equal when the variations are small (*5*).

Defining $\alpha_B = (1 + \epsilon_B) = (D/D_i)$, the binary diffusion coefficient ratio, the isotopic ratio at the injection site $x = 0$ is time independent and is given by $\delta_0 \approx \epsilon_B/2 =$ constant (*6*). The injection point lies in a symmetry plane for the ratio variation on $\pm x$ and is characterized by a heavy isotope enrichment, relative to the mean ratio, which is constant for all time in the "spike" injection model. Elsewhere the variation of the isotopic composition with x and t is related to variation in mixture concentration by

$$\left(\frac{\partial \lambda}{\partial \ln C}\right)_t = \epsilon_B \quad (5)$$

$$\left(\frac{\partial \lambda}{\partial \ln C}\right)_x = \epsilon_B \left[1 - \frac{t}{(x^2/2D)}\right]^{-\frac{1}{2}} \quad (6)$$

At any fixed time λ is a linear function of $\ln C$ with slope ϵ_B. For any fixed point x in the moving coordinate system, the right-hand side of Eq. 6 may be thought of as a local single-stage fractionation factor for the volume slice at x; plotted against time this function is a hyperbola with vertices ϵ_B, 0, and $-\epsilon_B$, x^2/D, and asymptotes 0 and $t = x^2/2D$. When ϵ_B is positive, then for times less than $x^2/2D$, the "local fractionation factor" at any point x is positive, increasing from ϵ_B at $t = 0$, to ∞, and R and C are both increasing. At times greater than $x^2/2D$ the "local factor" is negative, varying from $(-\infty)$ to 0 with increasing time, and R is increasing while C is decreasing as in familiar Rayleigh processes. For negative ϵ_B, R is decreasing at all time, but in both cases the heavy isotope concentration is increasing at all time except at $x = 0$.

In any instant of time the variation of mixture composition along the coordinate f is, from Eq. 4,

$$\lambda(x,t) = \ln \alpha_C - z^2(\alpha_C^2 - 1) \quad (7)$$

$$\delta(x,t) \approx \epsilon_C(1 - 2z^2) - (\epsilon_C z)^2(3 - 2z^2) \quad (8)$$

the latter equation being correct to second order. The characteristic fractionation factor in the carrier diffusion process is $\alpha_C = (1 + \epsilon_C) = (D/D_i)^{1/2}$. At $x = 0$, the composition is $\delta_0 = \epsilon_C \approx \epsilon_{B/2}$ for all time (*7*); at other points the composition is calculated along f via Eq. 3. At $f = 0$ and 1, δ goes to $(+\infty)$ or -1000 per mil, depending on the sign of ϵ_C, and the heavy isotope concentration goes to zero.

There are two values of f at which $\lambda = \delta = 0$ for all time, corresponding to $2z^2 \approx (1 - \epsilon_C)$ and occurring at $f^\dagger = 0.1587 + 0.12\ \epsilon_C$ and at $(1 - f^\dagger)$. These fractions are 17.1 and 82.9 percent for H_2-HD separation, and 15.2 and 84.8 percent for He^3-He^4 separation; for all other molecules except HT the values are almost precisely 16.0 and 84.0 percent. At these "zero-points" the ratio C/C_0 is $0.6065 + 0.30\epsilon_C$ for all time and the concentration is about 61 percent of that at the injection point $x = 0$; these points therefore characterize the fractionation pattern of the model in a distinctive fashion.

Figure 1 shows the calculated curve for $N^{15}N^{14}$-N_2^{14} separation in CO_2 carrier for the theoretical value $\epsilon_C = 5.3$ per mil, together with the experimental data (*3*), which are the δ values of seven equal fractions of the emerging gas. The theoretical curve correctly predicts the shape of the measured relationship and the two "zero-points" at $f = 15.9$ and 84.1 percent, where $\delta = 0$ and there is no fractionation relative to the original mixture. The exact prediction of the two "zero-points" shows that the theory is correct and that the fractionation takes place in the gas phase. However, the observed N^{15} enrichment is somewhat less than predicted in the central portion of the mixture and somewhat greater at the ends. The predicted curve is flattened in the manner expected for turbulent, non-fractionating, mixing between center and ends, presumably taking place after emergence from the rock but possibly also including some bulk mixing within the rock itself. This is a common effect in diffusive separation processes, resulting in an effective separation factor which is less than the theoretical maximum value calculated for pure diffusive separation.

The effective value of ϵ_C can be ob-

tained from the curve at $x = 0$, but if the symmetry is distorted by flow effects, a better way is to plot λ (or δ) against $-2z^2$; in such a plot both the slope and the intercept are equal to ϵ_C and δ should be zero at $2z^2 = 1$. The data in Fig. 1 are somewhat skewed, so that $2z^2$ is actually about 0.8, but a good fit is obtained with an effective $\epsilon_C = 3.0$ per mil, as shown in the figure. The measured data actually refer to finite fractions of 14.3 percent each; near the ends the calculated δ at the midpoint of a fraction will not be the same as the average of the fraction because the heavy isotope concentration goes to zero. When finite fraction intervals are collected it is therefore necessary to compare with the calculated mean δ values of such intervals. The concentration curve for species "i" is characterized by the variable $z_i = \alpha_C z$ and the corresponding fraction parameter $f_i = (1 + erf\ z_i)/2$. The mean isotope ratio in any interval f_1 to f_2, obtained by integrating the two concentration curves between z_1 and z_2, is

$$\frac{\bar{R}}{R^\dagger} = \frac{(f_2 - f_1)_i}{(f_2 - f_1)} \tag{9}$$

where the bar refers to the mean value for the fraction interval. The function $erf\ z_i = erf\ (z + \epsilon_C z)$ is obtained by Taylor expansion and, to second order, the result is

$$\bar{\delta} = \frac{-\epsilon_C}{(f_2 - f_1)} \times$$
$$[g(z_2)\ (1 - \epsilon_C z_2^2) - g(z_1)\ (1 - \epsilon_C z_1^2)] \tag{10}$$

$$g(z) = -\pi^{-\frac{1}{2}} z \exp(-z^2) \tag{11}$$

where $\bar{\delta}$ is the δ value of the finite fraction of mixture in the interval f_1 to f_2 ($f_2 > f_1$). The z values are obtained from Eq. 3 for the various values of f.

Calculated values for the composition of the seven equal N_2 fractions, using an effective ϵ_C value of 3.0 per mil, are compared with the observed data in Table 1. The standard deviation of observed points from calculated values is ± 0.4 per mil, which is the same as the experimental uncertainty (*3*). The local values of $\delta(f)$, calculated from Eq. 7, are 1.6 per mil greater (heavier) than the $\bar{\delta}$ interval values for fractions 1 and 7, 0.1 per mil greater for fractions 2 and 6, and no different for the other fractions. It should be noted that as f goes to 0 and 100 percent, δ goes to -1000 per mil as a limit when ϵ_C is positive, as in the present case. For negative ϵ_C as in He, δ goes to $(+\infty)$ at the ends, corresponding to infinite light isotope enrichment.

Table 1. Isotopic composition (δ in per mil) of seven equal fractions (14.3 percent intervals) of N_2 diffusing in CO_2, calculated for $\epsilon_c = 3.0$ per mil, and observed (*3*).

Fraction No.*	$\bar{\delta}N^{15}$ (calc.)	$\bar{\delta}N^{15}$ (obs.)
1	−5.0	−4.6
2	+1.0	+0.7
3	+2.6	+3.0
4	+3.0	+3.2
5	+2.6	+1.8
6	+1.0	+0.5
7	−5.0	−4.8

*No. 1 is the first fraction to emerge ($f = 0$ to 14.3 percent).

The simple "spike" model for carrier diffusion separation, with an effective separation factor approaching a predictable upper limit in the absence of mixing effects, accounts for the fractionation pattern observed in the Hoering-Moore experiment. A more sophisticated model, in which the injected mixture fills a finite space at $t = 0$, predicts a time-dependent enrichment at $x = 0$ with δ_0 growing from 0 at $t = 0$ to ϵ_C at infinite time (in the spike model δ_0 goes instantaneously to ϵ_C because the injection volume is infinitely small) (*8*). A study of the time dependence of δ_0 will show whether ϵ_C has been lowered by mixing effects or represents a transient value due to finite injection volume in particular experiments.

The fractions of interest for separating mixtures by carrier diffusion are the "double end-cut," consisting of the intervals 0 to f plus $(1 - f)$ to 1, and the center cut, containing the fraction intervals f to 0.5 and 0.5 to $(1 - f)$, obtained by splitting the emerging gas at f and $(1 - f)$ and combining the ends (f is taken as less than 50 percent). From Eq. 10 and material balance, the delta values for the material in the end and center cuts respectively are (*9*)

$$\bar{\delta}_E = -\epsilon_C g(z)/f \tag{12}$$

$$\bar{\delta}_O = +\epsilon_C g(z)/(0.5 - f) \tag{13}$$

It is important to note that f is the coordinate value at which the cut is made and *not* the size of the fraction. The double end-cut contains $2f$, and the center cut $(1 - 2f)$, of the material; correspondingly, z is $-erf^{-1}\ (1 - 2f)$ where f is the coordinate value of the cut.

In Fig. 2 the function $g\ (z)$ is plotted against $erf\ z$ for calculation of enrichments in finite fraction intervals. The f coordinate scale is folded back on itself at $x = 0$, so that f runs from 0.5 at $erf\ z = 0$, to 0 and 1 at $erf\ z = \pm 1$. The function $g\ (z)$ has a maximum at $erf\ z = \pm 0.682$, $z = \pm 2^{-\frac{1}{2}}$, corresponding to the "zero-points" at 16 and 84 percent, where $\delta = 0$. The composi-

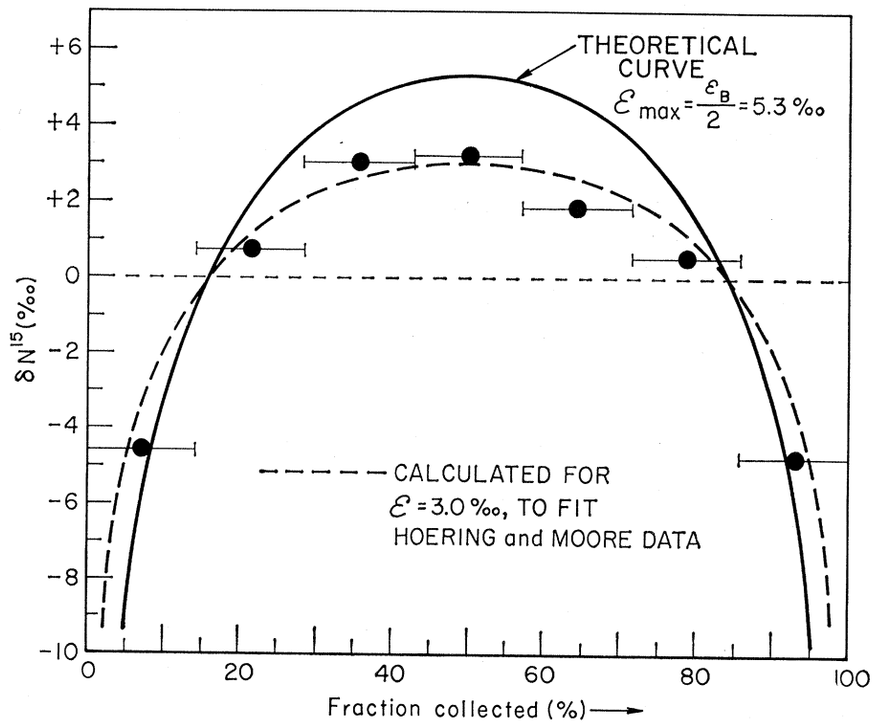

Fig. 1. Nitrogen isotope fractionation in CO_2 flowing through sandstone. Solid points are experimental values (*3*) for seven equal fractions (range of f shown by bars); since they represent finite fractions they fall below the calculated continuous curve in the first and last fraction.

tion of the end-cut at this point is $\bar{\delta}_E = -1.5\epsilon_C$. As f goes to zero it can be shown that the ratio $R/\bar{R}_E$ of the isotopic ratios in a slice at f and in the entire end-cut, is α_B, so that any slice is enriched in the heavy isotope by the binary diffusion coefficient ratio relative to all the material farther from the injection point.

Carrier diffusion enrichment may now be compared with that of the porous barrier or effusion process by writing the mean isotopic composition of the effluent cut from a barrier diffusion element, namely

$$\bar{\lambda}_P = \ln \{[1 - (1 - F)^{1/\alpha}]/F\} \quad (14)$$

$$\bar{\delta}_P \approx [\epsilon_P (1 - F) \ln (1 - F)]/\alpha F \quad (15)$$

where F is the fraction of input material which has effused from the element, $\bar{\delta}_P$ is its isotopic composition, and $\alpha = 1 + \epsilon_P$ is the fractionation factor for effusion $= (M_1/M)^{1/2}$. (The equation for $\bar{\delta}_P$ is always valid for F less than 0.5). Then let $F = 2f$ in order to compare light isotope (or more diffusible component) enrichment at the same total fraction of material obtained in the cut (that is, the double end-cut for carrier diffusion). The enrichment factors are related by $2\epsilon_C \approx \epsilon_P M_C/(M + M_C)$, so that the ratio of enrichments of a light isotope by the two processes is

$$\frac{\bar{\delta}_{CD}}{\bar{\delta}_{BD}} = \frac{-g(Z)}{(1 - F) \ln (1 - F)} \cdot \frac{M_C}{(M + M_C)} \quad (16)$$

in which CD and BD refer to carrier diffusion and barrier diffusion, F is the total fraction obtained in the cut, and $Z = -erf^{-1}(1 - F)$. As F goes to 0, $\bar{\delta}_{BD}$ goes to the single-stage factor $-\epsilon_P/\alpha$ while δ_{CD} goes to $(+\infty)$ or -1000 per mil, and the carrier diffusion enrichment becomes infinitely larger than for barrier diffusion.

For large values of M_C/M, carrier diffusion gives greater enrichments per stage for light isotopes (ϵ negative) for all cuts less than $F = 28.5$ percent ($f = 1/7$ in carrier diffusion, with the cut from each end combined as a double end-cut). The ratio $\bar{\delta}_{CD}/\bar{\delta}_{BD}$ is 1.8, 2.35, 3.1, and 3.7 at cuts of $F = 10$, 5, 2, and 1 percent respectively. For He^3 enrichment in CO_2 carrier (*7*), the carrier diffusion enrichments in the end-cut are $\bar{\delta}_E = 234$, 462, and 568 per mil at cuts of $F = 10$, 2, and 1 percent respectively, while the barrier diffusion enrichment approaches a limit of 151 per mil as F goes to zero. For U^{235} enrichment in UF_6, if a much heavier carrier could be found, $\epsilon_C = -2.15$ per mil and, for the same efficiency per stage, the number of stages required for a given enrichment would be 55 percent of those in barrier diffusion for cuts of $F = 10$ percent.

For heavy isotope (or less diffusible component) enrichment, the composition of residual mixture remaining in a porous barirer element is $\bar{\lambda}_{BD} = -(\epsilon_P/\alpha) \ln F' \approx \bar{\delta}_{BD}$, which can be compared with the composition of a center cut in carrier diffusion as given by Eq. 13. The ratio of enrichments is $\bar{\delta}_{CD}/\bar{\delta}_{BD} \approx [-g(Z')/F' \ln F'] \cdot [M_C/(M + M_C)]$ where F' is the center-cut fraction $(1 - 2f)$ remaining after removing the end-cuts at f and $(1 - f)$, and $Z' = -erf^{-1}(F')$. For M_C much greater than M, carrier diffusion produces greater enrichment per stage only for cuts of F' greater than 71.5 percent ($f < 1/7$), that is, for cuts so large that the barrier diffusion enrichment is less than one-third of ϵ_P. Thus carrier diffusion is not efficient for heavy isotope enrichment compared to effusion because, for better enrichments, the cuts are so large that the enrichment per stage becomes very small. Carrier diffusion is likely, therefore, to be most useful for concentration of rare isotopes lighter than the abundant species, and of H_2 and He in gas mixtures. Although the individual stages are injection points rather than elements with continuous flow, the stages are presumably subject to cascading with suitable carriers.

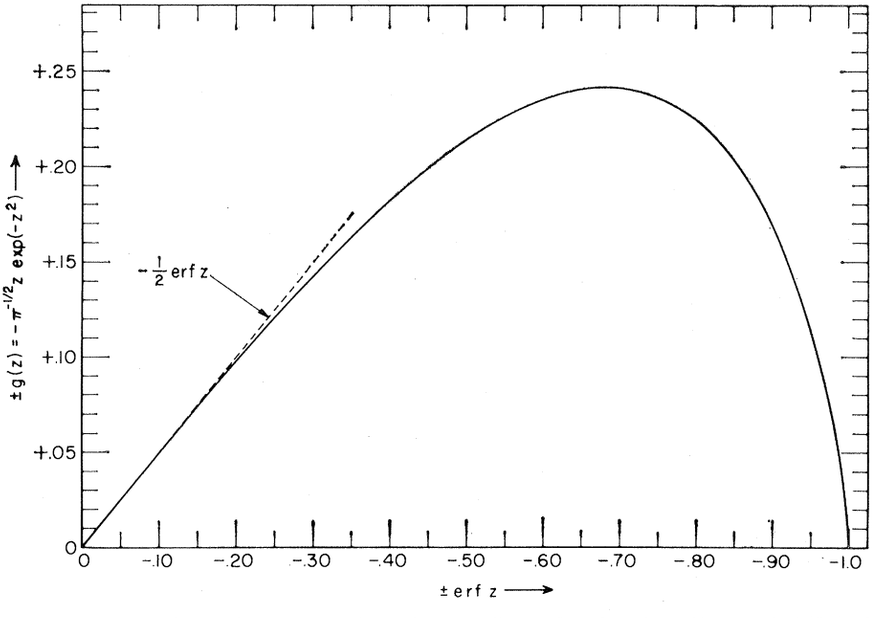

Fig. 2. The function $g(z)$ versus $erf\ z$. The coordinate fraction $f = (1 + erf\ z)/2$ is 0 and 1 at $erf\ z = \pm 1$, and 0.5 at $erf\ z = 0$.

H. CRAIG

Scripps Institution of Oceanography, La Jolla, California 92037

References and Notes

1. G. Hertz, *Z. Physik.* **19**, 35 (1923); **91**, 810 (1934); C. G. Maier, *J. Chem. Phys.* **7**, 854 (1939); M. Benedict and A. Boas, *Chem. Eng. Progr.* **47**, 51 and 111 (1951).
2. M. Cichelli, W. Weatherford, J. Bowman, *Chem. Eng. Progr.* **47**, 63 and 123 (1951).
3. T. Hoering and H. Moore, *Geochim. Cosmochim. Acta* **13**, 225 (1958).
4. F. Gazzarrini, R. Gonfiantini, and U. Colombo (personal communication) have found that C^{12}-C^{13} separation in CH_4 in a bentonite column with He carrier is dominated by the process described here.
5. Natural isotopic variations are reported by geochemists as δ values in per mil relative to isotopic standards.
6. D and D_1 are the binary diffusion coefficients for each component relative to the carrier gas when the mixture/carrier gas ratio is low enough that D_1 is not significantly affected by the presence of the abundant isotopic component of the mixture. The ratio $D/D_1 = \alpha_B$ is then simply $(M_1/M)^{\frac{1}{2}}[(M + M_C)/(M_1 + M_C)]^{\frac{1}{2}}$, the ratio of the reduced molecular masses for each isotopic species relative to the carrier gas of mass M_C. Note that ϵ_B can be positive or negative (because i always designates the *rare* isotope); δ_0 is negative if the light isotope is in low abundance as in He^3-He^4 mixtures but the *heavy* isotope concentrates at the injection point $x = 0$.
7. For H_2-HD and He^3-He^4 separation in CO_2, ϵ_C is 100.6 and −63.5 per mil respectively, while $\epsilon_B/2$ is 105.6 and −61.5 per mil. For all other compounds (except HT) ϵ_C is very close to $\epsilon_B/2$.
8. The finite-injection or "slug" model introduces another parameter, h, the half-length of the initial slug introduced at $x = 0$ between $x = \pm h$. The abundant species concentration is
$$C/C^\dagger = [erf\ (H - z) + erf\ (H + z)]/2$$
where $H = h/2\ (Dt)^{\frac{1}{2}}$ and $C^\dagger$ is the initial uniform concentration in the slug at $t = 0$. At $x = 0$ the concentration $C_0 = C^\dagger\ erf\ H$ and the isotopic composition is given by $\delta_0 \approx -2\epsilon_C\ g(H)/erf\ H$, where g is the function in Eq. 11 and $H = erf^{-1}\ (C_0/C^\dagger)$; δ_0 and H are both time dependent. The observed value of $\epsilon_C = 3$ per mil would correspond to transient values of $H = 0.85$ and $C_0/C^\dagger = 0.77$ in this model if mixing is not significant; in the experiment discussed (*3*) comparison of the two models cannot be made for lack of data.
9. The g functions in these and subsequent equations are to be multiplied by $(1-\epsilon_C z^2)$ when second-order precision is desired.
10. I thank Dr. Gazzarrini for stimulating the present study, which was supported by NSF.

28 September 1967